Nucleotide-binding oligomerization domain-containing protein 2 (Nod2) modulates T1DM susceptibility by gut microbiota

Running Title: Nod2 protects from T1DM by gut microbiota

Yang-yang Li[1,2*], James A. Pearson[1*], Chen Chao[1,3*], Jian Peng[1], Xiaojun Zhang[1], Zhiguang Zhou[3], Yu Liu[2,4], F. Susan Wong[5] and Li Wen[1,3]

[1]Section of Endocrinology, School of Medicine, Yale University, New Haven, Connecticut 06519, USA

[2]Department of Endocrinology, The 2nd Hospital of Jilin University, Changchun, Jilin, 130041, China

[3]Key Laboratory of Diabetes Immunology, Department of Metabolism and Endocrinology, The Second Xiangya Hospital, Central South University, Changsha, Hunan, 410011, China

[4] Department of Endocrinology, Sir Run Run Shaw Hospital, Nanjing Medical University, Nanjing, Jiangsu, 211100, China

[5]Diabetes Research Group, Institute of Infection and Immunity, School of Medicine, Cardiff University, Wales, CF14 4XN, UK

Correspondence to:

Li Wen
Section of Endocrinology
School of Medicine
Yale University
New Haven
Connecticut
USA
E-mail: li.wen@yale.edu
Telephone: 203.785.7186

* these authors contributed equally to the work

Word Count: 4253
Figures: 7 (+3 Supplemental)

Tables (1 Supplemental)

Abstract:

Nucleotide-binding oligomerization domain-containing protein 2 (Nod2) is an innate immune receptor. To investigate the role of Nod2 in susceptibility to the autoimmune disease, type 1 diabetes mellitus (T1DM), we generated *Nod2*$^{-/-}$ non-obese diabetic (NOD) mice. The *Nod2*$^{-/-}$NOD mice had different composition of the gut microbiota compared to *Nod2*$^{+/+}$NOD mice and were significantly protected from diabetes, but only when housed separately from *Nod2*$^{+/+}$NOD mice. This suggested that T1DM susceptibility in *Nod2*$^{-/-}$NOD mice is dependent on the alteration of gut microbiota, which modulated the frequency and function of IgA-secreting B-cells and IL-10 promoting T-regulatory cells. Finally, colonizing germ-free NOD mice with *Nod2*$^{-/-}$NOD gut microbiota significantly reduced pro-inflammatory cytokine-secreting immune cells but increased T-regulatory cells. Thus, gut microbiota modulate the immune system and T1D susceptibility. Importantly, our study raises a critical question about the housing mode in the interpretation of the disease phenotype of genetically-modified mouse strains in T1DM studies.

Key words: Type 1 diabetes mellitus; NOD; Nod2; Innate Immunity; Gut microbiota

1. Introduction:

Type 1 diabetes mellitus (T1DM) development is influenced by both genetic and environmental factors [1]. The incidence of T1DM has significantly increased worldwide [2-7] and environmental factors are thought to play a critical role in this. Innate immunity protects hosts from bacterial invasion by recognizing bacterial components through their pattern recognition receptors (PRRs). These PRRs include Toll-like receptors (TLRs) and nucleotide-binding oligomerization domain-like receptors (NOD-like receptors, NLRs). Interestingly, TLR deficiencies on the Non-Obese Diabetic (NOD) mouse background both increase susceptibility to and protect from T1DM [8-13]. Deficiency in MyD88, an adaptor protein that mediates most TLR signaling, induced complete protection from T1DM, which was abolished when *MyD88*$^{-/-}$NOD mice were housed in germ-free (GF) conditions [14]. Therefore, interactions between the TLR family and gut microbiota regulate T1DM development. However, much less is known about the role of NLR family members in T1DM susceptibility, in humans and mice. We recently reported that NLRP3, an important inflammasome component, influences T1DM development by regulating chemokines and their receptors in both immune cells and islet beta cells, preventing immune cell migration to the targeted tissue [15].

Nucleotide-binding oligomerization domain-containing protein 2 (Nod2) is a cytosolic bacterial sensor of muramyl dipeptide that induces antimicrobial peptide release and inflammatory signaling required for maintenance of the homeostasis of gut microbiota [16-18]. Nod2 mutations are associated with high susceptibility to Crohn's disease, a common inflammatory disorder of the bowel [19, 20]. Furthermore, Nod2 deficiency in

mice correlates with increased bacterial susceptibility [16, 21]. To investigate the role of Nod2 in a T1DM model, we generated NOD mice deficient in Nod2 (*Nod2*$^{-/-}$NOD). We hypothesized that Nod2 modulates T1DM development by regulating the composition of gut microbiota, which alters the immune cell function. Our results fully supported our hypothesis and raise an important point about alteration of immunological phenotype by housing conditions.

2. Materials and methods

2.1. Mice

NOD/Caj mice have been maintained at Yale University for approximately 30 years. *Nod2*$^{-/-}$B6 mice [16] were obtained from the Jackson Laboratory. They were backcrossed to NOD mice for 10 generations and the purity of the NOD genetic background was further confirmed by mouse genome scan (DartMouse). The mice were housed in specific pathogen-free (SPF) or germ-free (GF) conditions in a 12-hour dark/light cycle. All mice received irradiated food ad libitum and were housed in individually-ventilated filter cages (SPF) or open-topped cages within a gnotobiotic isolator (GF). Three types of experimental breeding and four types of experimental housing strategies were applied in this study as summarized in Supplementary Table 1. In the cohoused group (CH) equal numbers (2+2 or 3+3) of *Nod2*$^{+/+}$NOD and *Nod2*$^{-/-}$NOD mice were housed in the same cage, whereas non-cohoused (NCH) mice refers to *Nod2*$^{+/+}$NOD and *Nod2*$^{-/-}$NOD mice housed by genotype, i.e., *Nod2*$^{+/+}$NOD mice were only housed together with *Nod2*$^{+/+}$NOD and vice versa. The use of mice in this study was approved by the Institutional Animal Care and Use Committee at Yale University.

2.2. Natural history of diabetes development

Female *Nod2*$^{-/-}$NOD and *Nod2*$^{+/+}$NOD mice were assessed weekly for glycosuria for 30 weeks. Diabetes was confirmed by blood glucose of ≥250 mg/dL (≥13.9 mmol/L).

2.3. Short term and long term co-housing

Three to 4-week-old female *Nod2*$^{-/-}$NOD or *Nod2*$^{+/+}$NOD littermates were divided into groups, whereby *Nod2*$^{+/+}$NOD and *Nod2*$^{-/-}$NOD mice were housed in separate groups or co-housed in cages where the genotypes were mixed. Experiments were terminated when the mice were aged 9-10 weeks or 30 weeks old.

2.4. Histopathology and insulitis

Pancreata from 12-week old female mice were fixed in 10% buffered formalin and embedded in paraffin. Tissues were sectioned and stained with hematoxylin and eosin. Insulitis was scored under light microscopy with the following grading scale: 0, no insulitis; I, infiltration ＜25% of the islet; II, 25-75% infiltration; III, >75% infiltration. A range of 170–212 islets were scored for insulitis in each group (n = 7–8 mice). Significance was determined using a Chi square test. ** $p<0.01$.

2.5. Extraction of gut bacterial DNA

Fecal samples from female *Nod2*$^{-/-}$NOD and *Nod2*$^{+/+}$NOD mice were collected from 12-week old mice and resuspended in 300µl TE buffer containing 0.5% SDS and 200µg/ml Proteinase K. Bacterial DNA was extracted as previously described [22].

2.6. 16S rRNA sequencing and microbiota classification

The V4 region of the 16S rRNA gene was amplified from each DNA sample using a bar-coded broadly-conserved bacterial forward (5'-GTGCCAGCMGCCGCGGTAA-3') and reverse primer (5'-GGACTACHVGGGTWTCTAAT-3'). The PCR products were purified using a Qiagen gel extraction kit. The DNA concentration was quantified and equimolar amounts of each sample were pooled and used for pyrosequencing with the Ion Torrent PGM sequencing system (Life Technologies). The sequencing data were analyzed with the QIIME software package and UPARSE pipeline to pick operational taxonomic units (OTUs). Taxonomy assignment was performed using representative sequences of each OTU. Beta-diversity was calculated to compare differences between microbial communities, shown as Principal Coordinate Analysis (PCoA).

2.7. Quantitative real-time PCR (qPCR)

Quantitative real-time PCR (qPCR) was performed using Bio-Rad iQ5 qPCR detection system according to the manufacturer's instructions. The relative mRNA level of segmented filamentous bacteria (SFB) was determined using the 2-ΔΔCt method and normalization using the 16S rRNA values with SFB specific primers (forward primer:

5’-AGGAGGAGTCTGCGGCACATTAGC-3’ and reverse primer: 5’-TCCCCACTGCTGCCTCCCGTAG-3’).

2.8. Gut lumen IgA detection

Gut contents were collected from *Nod2*$^{+/+}$NOD and *Nod2*$^{-/-}$NOD mice at 12 weeks of age by flushing the small intestine with 10 mls of sterile PBS. The gut flush was then centrifuged (2000 rpm, 5mins, RT) and the supernatant was collected for IgA detection using ELISA (Southern Biotech) following the protocol described by Harriman et al [23].

2.9. Interaction of gut bacteria and immune cells in co-culture with splenocytes.

The large intestine was harvested from 2-month old female *Nod2*$^{-/-}$NOD and *Nod2*$^{+/+}$NOD mice and flushed with 5 mls of sterile PBS. The gut contents were vortexed for 2 mins followed by centrifuging for 5 mins at low speed (52xg) to remove dietary residue. The supernatant was transferred to a new tube and spun. After washing the pellet twice more, the combined supernatant was centrifuged at 469xg to remove mammalian cells. Bacteria in the supernatant were pelleted by centrifugation at high speed (1876xg, 5mins) and resuspended in PBS. Bacterial concentration was measured with a spectrophotometer (Bio-Rad) and heat-inactivated at 90℃ for 20 mins. 10^8 heat-inactivated bacteria were co-cultured with splenocytes ($2x10^6$/ml) from *Nod2*$^{-/-}$NOD or *Nod2*$^{+/+}$NOD mice for 14 hours prior to ICC.

2.10. Oral Gavage

Fresh fecal pellets were harvested from 4-5 week old *Nod2*$^{+/+}$NOD or *Nod2*$^{-/-}$NOD mice housed separately. Pellets were homogenized and gently centrifuged to remove large particles (1xg, 10 minutes). OD values were used to determine bacterial colony forming units (CFU). Germ-free WT NOD mice were then colonized with $2x10^8$ CFU by oral gavage, and terminated for experiments 2-3 weeks after gavage. Successful colonization was evaluated by 16S rRNA bacterial sequencing of fecal pellets from the ex-GF mice.

2.11. Antibodies and reagents

Briefly, cells were incubated with an Fc-blocking antibody (clone 2.4G2) at 4°C for 15mins, prior to surface staining. Antibodies to IgA (eBioscience; clone mA-6E1), IgG1 (BioLegend; clone RMG1-1), IgG2b (BioLegend; clone RMG2b-1), CD4 (BioLegend; clone GK1.5), CD8α (BioLegend; clone 53-6.7), CD19 (BioLegend; clone 6D5), B220 (BioLegend; clone RA3-6B2), TCRβ (BioLegend; clone H57-597), CD25 (BioLegend; clone 3C5) were used with viability determined using a Zombie Aqua™ Fixable Viability Kit (Biolegend). Treg cell staining was conducted using Tonbo Biosciences buffers (Foxp3/Transcription Factor Staining Buffer Kit; cat no: TNB-0607-KIT). Cells were stained as above, then fixed for 1 hour at RT prior to permeabilzation. The cells were then incubated with the 2.4G2 Fc-blocking antibody at 4°C for 15mins prior to staining with anti-FoxP3 PE (eBioscience; clone NRRF-30) for 30mins at 4°C. Hybridoma supernatants containing mAbs used for cell purification or stimulation, were generously provided by the

late Charles Janeway Jr. (Yale University). RPMI-1640 media and heat-inactivated FCS were purchased from Invitrogen and Gemini, respectively.

2.12. Cell surface and Intracellular cytokine (ICC) staining

Cells were stimulated with PMA (50ng/ml, Sigma) and ionomycin (500ng/ml, Sigma) in the presence of 1µl GolgiPlug^{TM} (BD) at 5x10^{6}/ml in cell culture medium for 4.5 hours. Fc receptors were blocked using the Fc-blocking antibody (incubated at 4°C for 15mins), then the cells were stained (30mins at 4°C) with surface markers and viability dye. The cells were then washed prior to fixation (20mins at RT) and permeabilization, using eBioscience^{TM} Intracellular fixation and permeabilization buffer set. The cells were then washed, blocked with the Fc-blocking antibody and then stained with anti-IFNγ (BioLegend; clone XMG1.2), anti-IL17a (BioLegend; clone TC11-18H10.1) and anti-TNFα (BioLegend; clone MP6-XT22) for 30mins at 4°C.

2.13. Treg suppression assays

Splenic and pancreatic lymph node (PLN)-derived Treg cells were isolated using Treg magnetic isolation kits (Stem cell technology, positive selection of $CD4^{+}CD25^{+}$ T-cells) and mitomycin-c-treated. Total NOD splenic APCs (post T-cell depletion and mitomycin-c-treatment) were used as alloantigen-stimulators. Purified splenic T cells from C57BL/6 mice were used as responders. Treg function was examined by suppression of the mixed lymphocyte reaction (MLR). Culture supernatants (to test secreted cytokines)

were collected on day 4 prior to ^{3}H-thymidine addition for the last 18 hours of the 5-day culture to assess proliferation.

2.14. Statistical analysis

Statistical analysis was performed using GraphPad Prism 7 software. Diabetes incidence was compared using log-rank test. *In vitro* assays were analyzed with Student's t test or ANOVA and $P<0.05$ was considered significant.

3. Results：

3.1. T1DM incidence in *Nod2*-deficient NOD mice was dependent on housing status

We set up three independent observation groups (summarized in Supplemental Table 1). Firstly, we investigated spontaneous diabetes in *Nod2*$^{-/-}$NOD mice and their co-housed (CH) *Nod2*$^{+/+}$NOD littermates (all females) over 30 weeks, from *Nod2*$^{+/-}$ breeding. We found that *Nod2*$^{-/-}$NOD mice developed diabetes similar to their WT littermates (Fig 1A). Secondly, to address the role of the gut microbiota (as Nod2 recognizes the bacterial component muramyl dipeptide) we set up another cohort of mice, in which *Nod2*$^{-/-}$NOD and their *Nod2*$^{+/+}$NOD female littermates from *Nod2*$^{+/-}$ breeding were separately housed (i.e. multiple mice of the same genotype were housed together) after weaning (non-cohoused, NCH). Interestingly, non-cohoused *Nod2*$^{-/-}$NOD mice showed significantly reduced T1DM development (31% vs. 71%, $p=0.003$, Fig. 1B). To confirm that the different

diabetes phenotype was due to the housing conditions, in a third set of experiments, the offspring from homozygous *Nod2*$^{-/-}$NOD breeding and homozygous *Nod2*$^{+/+}$NOD breeding were then co-housed after weaning at 3-4 weeks until 30 weeks old. *Nod2*$^{-/-}$NOD and *Nod2*$^{+/+}$NOD mice were housed separately as controls. Similar to the results shown in Fig. 1B, the non-cohoused *Nod2*$^{-/-}$NOD mice had significantly reduced T1DM incidence compared to non-cohoused *Nod2*$^{+/+}$NOD mice (33.3% vs. 86.7%, p=0.002, Fig. 1C). However, when the *Nod2*$^{-/-}$NOD and *Nod2*$^{+/+}$NOD mice were cohoused, the incidence of TIDM was increased in *Nod2*$^{-/-}$NOD mice and indistinguishable from the *Nod2*$^{+/+}$NOD counterparts, which had reduced incidence of diabetes (Fig. 1C). To assess disease severity, we also investigated the islet infiltration in 12-week old prediabetic mice and found that *Nod2*$^{-/-}$NOD mice had exacerbated islet infiltration when cohoused with WT *Nod2*$^{+/+}$NOD mice (Fig. 1D). These results suggested that the gut microbiota affected T1DM development.

3.2. Diabetes susceptibility is modulated by altered gut microbiota in *Nod2*-deficient NOD mice

We conducted further studies using non-littermate mice (from *Nod2*$^{-/-}$NOD breeding or *Nod2*$^{+/+}$NOD breeding) that were housed together (cohoused) or separately (non-cohoused) at weaning. We specifically did not use *Nod2*$^{-/-}$ and *Nod2*$^{+/+}$ littermates in order to study how distinct microbiota, shaped by *Nod2*, influence the immune responses. To verify whether gut microbiota were responsible for modifying T1DM susceptibility, we

collected fresh fecal samples from pre-diabetic female *Nod2*$^{-/-}$NOD and *Nod2*$^{+/+}$NOD mice and conducted 16S rRNA sequencing. Principal component analysis (PCA) revealed that the composition of gut microbiota from *Nod2*$^{-/-}$NOD mice was very different from *Nod2*$^{+/+}$NOD mice when they were not cohoused (Fig. 2A); however, this difference was eliminated upon cohousing the mice (Fig. 2B). We further evaluated changes of the microbiota composition at 3 weeks (before housing changes) and at 8-9 weeks of age (non-cohoused and cohoused). Interestingly, the gut microbiota composition was dramatically altered in *Nod2*$^{-/-}$NOD mice when cohoused compared to non-cohoused *Nod2*$^{-/-}$NOD mice, with the latter similar to the microbiota composition they had at 3 weeks whereas the former were indistinguishable from the microbiota composition of *Nod2*$^{+/+}$NOD mice (Supplemental Fig. 1A). Interestingly, *Nod2*$^{+/+}$NOD mice also had a change in their microbiota when they were cohoused or non-cohoused, although the change was much more subtle. This, however, suggests that the subtle changes in the microbiota of Nod2-sufficient mice over time may protect the mice from developing diabetes (Fig. 1C).

We identified that *Candidatus Arthromitus and Ruminococcus,* which are of the phylum Firmicutes, and *Adlercreutzia,* of the phylum Actinobacteria*,* were significantly increased in cohoused *Nod2*$^{-/-}$NOD mice compared with non-cohoused *Nod2*$^{-/-}$NOD mice (Fig. 2C, D, G). However, in the co-housed *Nod2*$^{+/+}$NOD mice there was a significantly decreased frequency of *Candidatus Arthromitus* compared to non-cohoused *Nod2*$^{+/+}$NOD mice (Fig. 2C). A similar trend was also noted in other genera including *Coprobacillus* (Fig. 2F). Interestingly, the effect of housing the mice had a stronger impact on the

microbiota compared with the *Nod2* gene effect, where only *Oscillospira* showed a trend towards a gene effect, being increased in *Nod2*$^{-/-}$NOD mice (Fig. 2E).

To test if SFB contribute to the disease protection in *Nod2*$^{-/-}$NOD, we examined the abundance of SFB by qPCR in the fecal samples of *Nod2*-deficient or *Nod2*-sufficient NOD mice both co-housed and housed separately. While there were no significant differences between non-cohoused and cohoused mice of the same *Nod2* genotype, there was a significant difference between non-cohoused *Nod2*$^{+/+}$NOD and *Nod2*$^{-/-}$NOD mice (Fig. 2H, $p < 0.05$), with higher levels of SFB in non-cohoused *Nod2*$^{+/+}$NOD mice. Together, our data suggest that the diabetes-protected phenotype found in *Nod2*$^{-/-}$NOD mice is mediated by gut microbiota and co-housing *Nod2*$^{-/-}$NOD and *Nod2*$^{+/+}$NOD mice can alter the composition of gut microbiota, leading to a change in diabetes phenotype. However, our data show a reduction of SFB in the protected mice, thus do not support a protective role of SFB in diabetes development in these mice.

Nod2-deficiency has been shown to reduce the level of antimicrobial peptides (AMPs) and thus alter the gut microbiota in other models [16, 18]. Therefore, we investigated whether AMPs contribute to the altered gut microbiota composition in *Nod2*$^{-/-}$NOD and *Nod2*$^{+/+}$NOD mice, both cohoused and non-cohoused. As expected, non-cohoused *Nod2*$^{-/-}$NOD mice had reduced levels of AMPs (particularly Reg3β) compared to non-cohoused *Nod2*$^{+/+}$NOD mice (Supplemental Fig. 1B-D). Further, cohousing significantly increased AMP levels, as others have previously reported [24]. This suggests that alterations in AMP expression were at least partly responsible for the altered microbiota.

3.3. Effect of Nod2 on macrophages (Mϕ) and dendritic cells (DCs)

We next examined the phenotype of the immune cells from cohoused and non-cohoused mice. As antigen presenting cells (APCs), especially Mϕ and DCs, are able to take up and present antigens from the gut lumen [25, 26], we hypothesized that APCs contributed to the modulation of T1DM susceptibility associated with Nod2. However, the frequency and phenotype of $CD11b^+$ Mϕ or $CD11c^+$ DCs in WT and *Nod2*-deficient NOD mice were comparable, regardless of the housing conditions (data not shown). We then tested the function of Mϕ and DCs using purified $CD11b^+$ and $CD11c^+$ populations from $Nod2^{+/+}$NOD and $Nod2^{-/-}$NOD mice. There were no obvious differences in APC function, assessed by stimulation of diabetogenic $CD4^+$ BDC2.5 T-cells or $CD8^+$ NY8.3 T-cells *in vitro* between $Nod2^{-/-}$NOD or $Nod2^{+/+}$NOD mice (Supplementary Fig. 2A and B). Finally, we tested the Mϕ and DCs *in vivo*, in adoptive transfer experiments in immune-deficient hosts. We transferred diabetogenic T-cells, from diabetic $Nod2^{+/+}$NOD mice, to $Nod2^{-/-}$ and $Nod2^{+/+}$ NOD.scid mice and evaluated diabetes development in the recipients. In line with our *in vitro* results, endogenous Mϕ and DCs in *Nod2*-sufficient or deficient NOD.scid mice did not affect the incidence of diabetes in the recipients (Supplementary Fig 2C). These results suggest that the Mϕ and DCs are not responsible for altered Nod2-mediated spontaneous diabetes susceptibility, unlike the streptozotocin-induced model [27].

3.4. Effect of Nod2 on mucosal B-cells

We hypothesized that *Nod2* may affect B-cell function, particularly IgA-producing B-cells. Therefore, we investigated the proportion of IgA^+ B-cells in the Peyer's patches (PPs). While there was a comparable proportion of IgA-producing B-cells in PPs of *Nod2*$^{-/-}$NOD and *Nod2*$^{+/+}$NOD mice when housed separately (Fig. 3A), co-housing led to a significant increase of IgA-producing B-cells in PPs of *Nod2*$^{-/-}$NOD mice. A similar trend was also seen in cohoused *Nod2*$^{+/+}$NOD mice (Fig. 3A). An increase in secreted IgA was also detected in the small intestine (Fig. 3B). This suggests that the cohousing induced altered gut microbiota, which in turn promoted mucosal B-cell responses, whereas in the steady state of gut microbiota, IgA-producing mucosal B-cells were not affected by Nod2. PP-residing IgG2b-expressing B-cells were also influenced by cohousing, as non co-housed *Nod2*$^{-/-}$NOD mice had lower levels of IgG2b-expressing B-cells compared to co-housed *Nod2*$^{-/-}$NOD mice (Fig. 3C). Further, IgG1-expressing B-cells were increased in CH WT *Nod2*$^{+/+}$NOD mice when compared to CH *Nod2*$^{-/-}$NOD mice within the PP (Fig. 3D). Together, these data suggest that the altered microbiota induced by cohousing affect the mucosal antibody responses.

3.5. Effect of Nod2 on T-cells

To investigate if Nod2 affects T-cell function, we examined cytokine expression of T-cells from spleen, PLN and PPs. We found that, in the absence of Nod2, co-housing led to a significant increase of IFNγ-producing $CD8^+$ T-cells in PPs of *Nod2*$^{-/-}$NOD mice compared with non-cohoused *Nod2*$^{-/-}$NOD or cohoused *Nod2*$^{+/+}$ NOD mice (Fig. 4A).

Interestingly, a lower percentage of splenic IL-17A-producing $CD4^+$ T-cells was seen in *Nod2*$^{-/-}$NOD mice whereas co-housing significantly increased the percentage of IL-17A-producing $CD4^+$ T-cells in PLN and PPs of *Nod2*$^{-/-}$NOD mice compared with non-cohoused *Nod2*$^{-/-}$NOD or *Nod2*$^{+/+}$NOD mice (Fig. 4B). SFB have been shown to induce IL17-expressing T cells [28]. Interestingly, the $CD4^+IL17a^+$ T cells showed a similar pattern to the level of SFB detected (Fig 2H), particularly splenic $CD4^+IL17a^+$ T cells (Fig. 4B). The increased proportion of IL17-expressing $CD4^+$ T cells in both the PLN and PP from cohoused *Nod2*$^{-/-}$NOD mice that had increased diabetes suggests that other microbiota are capable of inducing IL17 in CD4 T cells.

Next we investigated whether housing conditions affect Tregs. We found proportional changes in $CD4^+CD25^+FoxP3^+$ T-cells predominantly in the PLNs (Fig. 5A and B). Interestingly, the *Nod2*$^{+/+}$NOD mice housed separately, which have the highest incidence of diabetes, had the lowest proportion of Tregs. Further, the *Nod2*$^{+/+}$NOD co-housed with *Nod2*$^{-/-}$NOD mice (which reduced diabetes onset) or the *Nod2*$^{-/-}$NOD mice housed separately (which have the lowest incidence of diabetes), had the highest proportions of Tregs. Our results suggested a role of the gut microbiota in inducing Tregs (Fig. 5A). To assess Treg function, we performed suppression assays using MLRs, in which T-cells from C57BL/6 mice (responders) were co-cultured with mitomycin-c treated NOD APCs (stimulators) in the presence of purified Treg cells (suppressors) from *Nod2*$^{+/+}$NOD and *Nod2*$^{-/-}$NOD mice (housed together or separately). We found significant suppression of the proliferation of responder cells in the presence of Treg cells at 1:3 Treg:Tresponder ratio (Fig. 5C), although no suppression was observed at a 1:10 ratio (data not shown). Thus,

housing status, which altered gut microbiota, affected both the number and function of the Treg cells. Secreted cytokines in the supernatants of the Treg suppression assays revealed a significant increase in anti-inflammatory IL-10, associated with Nod2 deficiency (Fig. 5D). Similar results were seen in an autoantigen-specific Treg suppression assay (data not shown).

3.6. Direct effect of gut microbiota on T-cell function

To confirm if the housing-dependent change in gut microbiota was responsible for the different immune responses in the *Nod2*$^{-/-}$NOD mice, we stimulated splenocytes from 2-month old female *Nod2*$^{-/-}$NOD and *Nod2*$^{+/+}$NOD mice with heat-inactivated colonic bacteria of *Nod2*$^{-/-}$NOD or *Nod2*$^{+/+}$NOD mice. Similar to the ICC staining shown (Fig. 4), there was a significant reduction of IFN-γ producing CD8^{+} T-cells from *Nod2*$^{-/-}$NOD mice when compared to *Nod2*$^{+/+}$NOD mice, in response to gut bacteria from either *Nod2*-deficient or sufficient mice (Fig. 6A). However, gut bacteria from *Nod2*$^{+/+}$NOD mice induced a greater IFN-γ production from CD8^{+} T-cells from *Nod2*$^{-/-}$NOD or *Nod2*$^{+/+}$NOD mice (Fig. 6A), indicating that gut bacteria from *Nod2*$^{+/+}$NOD mice are more inflammatory. Interestingly, the gut bacteria, regardless of the donor, appeared to suppress IL-17A-producing CD4^{+} T-cells (Fig. 6B) and we did not find direct effects of gut bacteria on TNF-α or IL-10-producing T-cells *in vitro* (data not shown).

Taken together, our results suggest *Nod2*$^{-/-}$NOD mice had a distinct gut microbiota composition compared with *Nod2*$^{+/+}$NOD mice, and that the variance in components of gut microbiota altered the immune cell function which modulates T1DM susceptibility.

To further prove the concept, we colonized germ-free (GF) NOD mice with feces from 4-5 week old *Nod2*$^{-/-}$NOD or *Nod2*$^{+/+}$NOD mice that were housed separately. We studied the ex-GF mice 2-3 weeks after introduction of gut bacteria. 16S rRNA sequencing results showed a clear separation in the recipients depending on the donor microbiota they received (Fig. 7A). Interestingly, we found increased cecal weight in the ex-GF mice given *Nod2*$^{-/-}$NOD feces (Supplemental Fig. 3A) and the small intestine was also longer (data not shown), neither of which were observed in SPF *Nod2*$^{-/-}$NOD mice (data not shown). We also found reduced inflammatory cytokine-producing B cells, T cells in PLNs of ex-GF mice colonized with *Nod2*$^{-/-}$NOD fecal bacteria (Fig. 7B). In line with the reduction of inflammatory cytokine production by immune cells, these mice also had a higher frequency and absolute number of $CD4^+CD25^+FoxP3^+$ Treg cells in the mesenteric lymph nodes (MLNs) and PPs compared to their counterparts colonized with *Nod2*$^{+/+}$NOD fecal bacteria (Fig. 7C-E).

There were no changes in phenotype and cytokine production in DCs or Mϕ in the ex-GF mice (data not shown). However, given the results of the changes in IgA^+ B-cells in cohoused SPF *Nod2*$^{-/-}$NOD mice and altered cytokine production in the ex-GF mice colonized with *Nod2*$^{-/-}$NOD fecal bacteria (Fig. 3 and 7B), we tested islet-specific APC function of the B-cells in these conventionalized GF mice. Supporting the immune tolerant status of these B-cells, B-cells from the ex-GF mice colonized with *Nod2*$^{-/-}$NOD fecal

bacteria showed attenuated antigen presentation to both BDC2.5 $CD4^+$ T-cells and NY8.3 $CD8^+$ T-cells compared to the B-cells from the ex-GF mice colonized with *Nod2*$^{+/+}$NOD bacteria (Supplementary Fig. 3B-C). Taken together, we provide evidence that Nod2 alters the composition of gut microbiota, which in turn modulate the adaptive immune system and influence diabetes susceptibility.

4. Discussion:

Our study sought to understand the role Nod2 plays in the development of spontaneous T1DM susceptibility. Our key finding was that Nod2-mediated T1DM susceptibility was dependent on the composition of the gut microbiota, which could be influenced by the housing of *Nod2*-deficient or sufficient NOD mice. The *Nod2*-deficient NOD mice were protected from T1DM development, if they were housed only with *Nod2*-deficient NOD mice. However, the disease protection was diminished if they were housed with *Nod2*-sufficient littermates. Conversely, the higher incidence of the *Nod2*-sufficient NOD mice was reduced when these mice were housed with their *Nod2*-deficient NOD littermates, emphasizing the importance of gut bacteria in influencing diabetes incidence. This was further confirmed by housing *Nod2*-deficient mice with *Nod2*-sufficient non-littermate mice. Although Nod2 deficiency led to a distinctive community of gut microbiota in NOD mice, its effect on diabetes was masked by the dominant community from *Nod2*-sufficient mice when cohoused. Thus, one of the roles of the *Nod2* gene in T1DM development was to alter the gut microbiota. While macrophages and DCs were unaffected by Nod2 deficiency, the phenotype and functions of T- and B-cells were altered, some of which was likely to be

related to the gut microbiota composition. This suggests that Nod2 activation is important for mediating changes in the gut microbiota, which affects the adaptive immune cells and subsequently diabetes development.

We recently showed that NLRP3 alters T1DM development by limiting the recruitment and infiltration of autoreactive $CD4^+$ T-cells into the pancreas [15]. Our current study provides evidence that NLR signaling is important for modulating diabetes susceptibility by alteration of the microbial composition, which in turn affects the phenotype and functions of immune cells. Furthermore, this study demonstrates that the *Nod2* gene effect on T1DM susceptibility is due to altering the composition of gut microbiota, and diabetes protection in *Nod2*-deficient mice is dependent on the gut microbial conditioning. This was supported by the results from three sets of experiments: i) cohousing $Nod2^{-/-}$NOD with $Nod2^{+/+}$NOD mice, littermates or non-littermates, ii) investigating the role of Nod2 in non-cohoused $Nod2^{-/-}$NOD mice, in which diabetes development was significantly reduced; iii) reconstitution of gut microbiota from $Nod2^{-/-}$NOD or $Nod2^{+/+}$NOD to germ-free NOD mice.

The diabetes incidence differences in $Nod2^{-/-}$NOD mice, when living with different housing partners, strongly supports the role of gut microbiota. We found a distinct profile of the gut microbiota between $Nod2^{-/-}$NOD and $Nod2^{+/+}$NOD mice when they are housed separately, which correlated with diabetes development. It is known that Nod2 is important for the expression of antimicrobial peptides and in controlling the expansion of intestinal bacteria [16, 18]. In line with those reports, we found Nod2-deficient NOD mice expressed reduced levels of antimicrobial peptides; however, upon cohousing with Nod2-sufficient NOD mice, the levels of AMPs were increased. This suggests that the

secretion of antimicrobial peptides is gut microbiota-dependent but can be independent of Nod2, as others have reported [24]. Therefore, the alterations of gut microbiota composition in the *Nod2*$^{-/-}$NOD mice, caused by cohousing with *Nod2*$^{+/+}$NOD mice, induce a large increase in AMP synthesis to similar levels seen in the Nod2-sufficient mice, thereby, diminishing diabetes protection in Nod2-deficient mice.

Interestingly, Nod2 deficiency had no effect on professional APCs, such as macrophages or DCs. However, the APC function of B-cells was attenuated in the absence of Nod2 or in the presence of *Nod2*$^{-/-}$NOD gut microbiota. Nod2 deficiency also altered IgA-producing B-cells. It is well documented that a large amount of IgA is secreted into the gut lumen to protect the host from microbial invasion [29-31]. In Nod2 deficiency, a mild reduction of secreted IgA in gut lumen was observed; however, cohousing with *Nod2*$^{+/+}$NOD mice significantly promoted IgA production into the gut lumen. This indicated that the gut microbiota tightly regulate the intestinal immune system in response to the newly-introduced gut bacteria by cohousing. Cohousing of *Nod2*$^{-/-}$NOD mice with *Nod2*$^{+/+}$NOD mice also affected pro-inflammatory cytokine-producing T cells and Treg cells in the lymphoid tissue outside the intestine including PLN. This indicates that PLN have an intimate relationship with gut mucosal immunity. Turley has reported that PLNs drain antigens from both pancreas and intestine [32]. In line with this observation, we recently found a commensal microbial antigen that can be recognized by diabetogenic T cells, which in turn attack islet beta cells [33]. Similar results were also observed in an autoimmune uveitis model [34]. It is conceivable that *Nod2*$^{-/-}$NOD mice harbor less diabetogenic gut microbiota, and thereby have a lower frequency of proinflammatory

cytokine-producing T-cells but a higher frequency of Treg cells in PLNs. However, more immunostimulatory gut microbiota were present in *Nod2*$^{-/-}$NOD mice after cohousing with WT mice, which led to a higher frequency of proinflammatory cytokine-producing T-cells and increased disease onset. The proof of concept using GF mice confirmed our hypothesis.

Costa reported recently that Nod2 is important in streptozotocin-induced diabetes in C57BL/6 mice [27]. Although both our study and theirs demonstrated increased Tregs in response to *Nod2*$^{-/-}$ microbiota, the cause of the Treg increase in the two model systems was different. In our spontaneous T1DM model, gut microbiota affected by housing status, regulated the change of Tregs; however, the anti-inflammatory cytokine IL-10 production was regulated by Nod2 gene expression (or lack of expression) but independent of housing conditions. While Costa and colleagues showed that $CD11b^{+}CD11c^{+}$ cells were important for mediating suppression and diabetes protection in their streptozotocin-induced disease model, we did not observe any changes in both phenotype and function of DCs or macrophages *in vitro* and *in vivo*. The changes we observed were in the B and T-cells in our spontaneous diabetes model. The discrepancy between the two studies was most likely due to the two very different model systems, streptozotocin-induced diabetes and spontaneous T1DM. More importantly, the two studies also used two very different mouse strains with different genetic backgrounds, C57BL/6 vs NOD.

Our study also raises a very important issue of housing conditions in interpretation of the disease phenotype in a genetically-targeted mouse strain. We propose that the phenotype should be tested in two housing conditions – cohousing with gene-sufficient

littermates and housing separately from gene-sufficient mice. If the disease phenotype is affected by the housing conditions when housed separately, as in our study, but not when cohoused, it suggests that the change in the gut microbiota is an integral part of the effect exerted by the specific gene.

Although the mouse Nod2 protein shares high homology with human Nod2 protein [35], it is not known if *Nod2* has genetic associations with human T1D. However, a recent study suggests a high prevalence of inflammatory bowel disease (IBD) in patients with T1D [36]. It is not clear whether the patients developed IBD first or T1D first; however, *Nod2* is a major susceptibility gene for IBD [19, 20] and Nod2 plays an important role in mediating microbial signaling responses. It is possible that activation of Nod2 pathway may be context-dependent in individuals with T1D, i.e., dependent on microbial exposure, as we found in NOD mice.

In conclusion, our data suggest that Nod2 plays a role in T1DM development. Unlike inflammatory bowel disease, where the *Nod2* gene plays a dominant role in the disease development, in T1DM, the role of the *Nod2* gene contributes to alteration of the gut microbiota, but this effect can be over-ridden by altering the housing conditions. Thus, Nod2 acts as a recessive modulator in T1DM susceptibility. Finally, as human T1D incidence is increasing, this adds further weight to the increased importance of environmental factors in human studies.

Author Contributions

YYL, JAP, FSW and LW designed the experiments; YLi, JAP, CC, JP and XZ carried out experiments; YYL, JAP, JP, FSW and LW analyzed data, ZZ, YL, FSW and LW supervised the study; YYL, JAP, FSW and LW wrote the manuscript. The project was conceived by LW, who assumes responsibility for the work.

Acknowledgements

We thank Karl Hager (Lab Medicine, Yale) for assistance with 16S rRNA sequencing and all the lab members for their kind technical help and critical scientific comments during the study.

Funding

This work was supported by NIH (DK092882, DK100500, and P30 DK945735 to LW), by ADA (1-14-BS-222) to LW and a Fulbright-Diabetes UK Research scholarship and a JDRF postdoctoral fellowship to J.A.P. There are no conflicts of interest to disclose.

References:

[1] T. Tuomi, N. Santoro, S. Caprio, M. Cai, J. Weng, L. Groop. The many faces of diabetes: a disease with increasing heterogeneity. Lancet, 2014;383**:**1084-94.

[2] Variation and trends in incidence of childhood diabetes in Europe. EURODIAB ACE Study Group. Lancet, 2000;355**:**873-6.

[3] K. M. Gillespie, S. C. Bain, A. H. Barnett, P. J. Bingley, M. R. Christie, G. V. Gill *et al.* The rising incidence of childhood type 1 diabetes and reduced contribution of high-risk HLA haplotypes. Lancet, 2004;364**:**1699-700.

[4] K. Bessaoud, G. Boudraa, M. Molinero de Ropolo, M. de Sereday, M. L. Marti, M. Moser *et al.* Incidence and trends of childhood Type 1 diabetes worldwide 1990-1999. Diabetic Medicine, 2006;23**:**857-66.

[5] V. Harjutsalo, L. Sjöberg, J. Tuomilehto. Time trends in the incidence of type 1 diabetes in Finnish children: a cohort study. Lancet, 2008;371**:**1777-82.

[6] J. Evertsen, R. Alemzadeh, X. Wang. Increasing Incidence of Pediatric Type 1 Diabetes Mellitus in Southeastern Wisconsin: Relationship with Body Weight at Diagnosis. Plos One, 2009;4:e6873.

[7] S. Ehehalt, K. Dietz, A. M. Willasch, A. Neu, I. Baden-Wuerttemberg Daibet. Epidemiological Perspectives on Type 1 Diabetes in Childhood and Adolescence in Germany - 20 years of the Baden-Wurttemberg Diabetes Incidence Registry (DIARY). Diabetes Care, 2010;33**:**338-40.

[8] H. S. Kim, M. S. Han, K. W. Chung, S. Kim, E. Kim, M. J. Kim *et al.* Toll-like receptor 2 senses beta-cell death and contributes to the initiation of autoimmune diabetes. Immunity, 2007;27**:**321-33.

[9] F. S. Wong, C. Hu, L. Zhang, W. Du, L. Alexopoulou, R. A. Flavell *et al.* The role of Toll-like receptors 3 and 9 in the development of autoimmune diabetes in NOD mice. Ann N Y Acad Sci, 2008;1150**:**146-8.

[10] Y. Zhang, A. S. Lee, A. Shameli, X. Geng, D. Finegood, P. Santamaria *et al.* TLR9 blockade inhibits activation of diabetogenic CD8+ T cells and delays autoimmune diabetes. J Immunol, 2010;184**:**5645-53.

[11] D. H. Kim, J. C. Lee, M. K. Lee, K. W. Kim, M. S. Lee. Treatment of autoimmune diabetes in NOD mice by Toll-like receptor 2 tolerance in conjunction with dipeptidyl peptidase 4 inhibition. Diabetologia, 2012;55**:**3308-17.

[12] E. Gülden, M. Ihira, A. Ohashi, A. L. Reinbeck, M. A. Freudenberg, H. Kolb *et al.* Toll-like receptor 4 deficiency accelerates the development of insulin-deficient diabetes in non-obese diabetic mice. PLoS One, 2013;8**:**e75385.

[13] N. Tai, F. S. Wong, L. Wen. TLR9 deficiency promotes CD73 expression in T cells and diabetes protection in nonobese diabetic mice. J Immunol, 2013;191**:**2926-37.

[14] L. Wen, R. E. Ley, P. Y. Volchkov, P. B. Stranges, L. Avanesyan, A. C. Stonebraker *et al.* Innate immunity and intestinal microbiota in the development of Type 1 diabetes. Nature, 2008;455**:**1109-13.

[15] C. Hu, H. Ding, Y. Li, J. A. Pearson, X. Zhang, R. A. Flavell *et al.* NLRP3 deficiency protects from type 1 diabetes through the regulation of chemotaxis into the pancreatic islets. *Proc Natl Acad Sci U S A*; 2015;112:11318-23.

[16] K. S. Kobayashi, M. Chamaillard, Y. Ogura, O. Henegariu, N. Inohara, G. Nuñez *et al.* Nod2-dependent regulation of innate and adaptive immunity in the intestinal tract. Science, 2005;307**:**731-4.

[17] A. Biswas, Y. J. Liu, L. Hao, A. Mizoguchi, N. H. Salzman, C. L. Bevins *et al.* Induction and rescue of Nod2-dependent Th1-driven granulomatous inflammation of the ileum. Proc Natl Acad Sci U S A, 2010;107**:**14739-44.

[18] D. Ramanan, M. S. Tang, R. Bowcutt, P. Loke, K. Cadwell. Bacterial sensor Nod2 prevents inflammation of the small intestine by restricting the expansion of the commensal Bacteroides vulgatus. Immunity, 2014;41**:**311-24.

[19] Y. Ogura, D. K. Bonen, N. Inohara, D. L. Nicolae, F. F. Chen, R. Ramos *et al.* A frameshift mutation in NOD2 associated with susceptibility to Crohn's disease. Nature, 2001;411**:**603-6.

[20] J. P. Hugot, M. Chamaillard, H. Zouali, S. Lesage, J. P. Cézard, J. Belaiche *et al.* Association of NOD2 leucine-rich repeat variants with susceptibility to Crohn's disease. Nature, 2001;411**:**599-603.

[21] M. Divangahi, S. Mostowy, F. Coulombe, R. Kozak, L. Guillot, F. Veyrier *et al.* NOD2-deficient mice have impaired resistance to Mycobacterium tuberculosis infection through defective innate and adaptive immunity. J Immunol, 2008;181**:**7157-65.

[22] J. Peng, S. Narasimhan, J. R. Marchesi, A. Benson, F. S. Wong, L. Wen. Long term effect of gut microbiota transfer on diabetes development. J Autoimmun, 2014;53**:**85-94.

[23] G. R. Harriman, D. Y. Kunimoto, J. F. Elliott, V. Paetkau, W. Strober. The role of IL-5 in IgA B cell differentiation. J Immunol, 1988;140**:**3033-9.

[24] M. T. Shanahan, I. M. Carroll, E. Grossniklaus, A. White, R. J. von Furstenberg, R. Barner *et al.* Mouse Paneth cell antimicrobial function is independent of Nod2. Gut, 2014;63**:**903-10.

[25] J. R. McDole, L. W. Wheeler, K. G. McDonald, B. Wang, V. Konjufca, K. A. Knoop *et al.* Goblet cells deliver luminal antigen to CD103+ dendritic cells in the small intestine. Nature, 2012;483**:**345-9.

[26] J. Farache, I. Koren, I. Milo, I. Gurevich, K. W. Kim, E. Zigmond *et al.* Luminal bacteria recruit CD103+ dendritic cells into the intestinal epithelium to sample bacterial antigens for presentation. Immunity, 2013;38**:**581-95.

[27] F. R. Costa, M. C. Françozo, G. G. de Oliveira, A. Ignacio, A. Castoldi, D. S. Zamboni *et al.* Gut microbiota translocation to the pancreatic lymph nodes triggers NOD2 activation and contributes to T1D onset. J Exp Med, 2016;213**:**1223-39.

[28] I. I. Ivanov, K. Atarashi, N. Manel, E. L. Brodie, T. Shima, U. Karaoz *et al.* Induction of intestinal Th17 cells by segmented filamentous bacteria. Cell, 2009;139**:**485-98.

[29] M. W. Russell, T. A. Brown, J. L. Claflin, K. Schroer, J. Mestecky. Immunoglobulin A-mediated hepatobiliary transport constitutes a natural pathway for disposing of bacterial antigens. Infect Immun, 1983;42**:**1041-8.

[30] P. P. Jonard, J. C. Rambaud, C. Dive, J. P. Vaerman, A. Galian, D. L. Delacroix. Secretion of immunoglobulins and plasma proteins from the jejunal mucosa. Transport rate and origin of polymeric immunoglobulin A. J Clin Invest, 1984;74**:**525-35.

[31] A. Phalipon, A. Cardona, J. P. Kraehenbuhl, L. Edelman, P. J. Sansonetti, B. Corthésy. Secretory component: a new role in secretory IgA-mediated immune exclusion in vivo. Immunity, 2002;17**:**107-15.

[32] S. J. Turley, J. W. Lee, N. Dutton-Swain, D. Mathis, C. Benoist. Endocrine self and gut non-self intersect in the pancreatic lymph nodes. Proc Natl Acad Sci U S A, 2005;102**:**17729-33.

[33] N. Tai, J. Peng, F. Liu, E. Gulden, Y. Hu, X. Zhang *et al.* Microbial antigen mimics activate diabetogenic CD8 T cells in NOD mice. J Exp Med, 2016;213**:**2129-46.

[34] R. Horai, C. R. Zárate-Bladés, P. Dillenburg-Pilla, J. Chen, J. L. Kielczewski, P. B. Silver *et al.* Microbiota-Dependent Activation of an Autoreactive T Cell Receptor Provokes Autoimmunity in an Immunologically Privileged Site. Immunity, 2015;43**:**343-53.

[35] A. L. Pauleau, P. J. Murray. Role of nod2 in the response of macrophages to toll-like receptor agonists. Mol Cell Biol, 2003;23**:**7531-9.

[36] H. A. Penny, J. S. Leeds, M. Kurien, A. Averginos, A. D. Hopper, M. Hadjivassiliou *et al.* The relationship between inflammatory bowel disease and type 1 diabetes mellitus: a study of relative prevalence in comparison with population controls. J Gastrointestin Liver Dis, 2015;24**:**125-6.

Figure legends

Fig. 1 - Diabetes development in *Nod2*$^{-/-}$NOD mice is dependent on housing status.

(A), Diabetes development was observed in female *Nod2*$^{-/-}$NOD and *Nod2*$^{+/+}$NOD mice that were reared together (CH, co-housed) or (B) separated by genotype (NCH, non-cohoused). (C), Diabetes development was observed in female *Nod2*$^{-/-}$NOD and *Nod2*$^{+/+}$NOD mice that were born from different mothers and either the strains were cohoused post-weaning (CH) or housed with littermates of their own genotype (NCH). Mice were screened weekly for glycosuria and confirmed by blood glucose ＞250 mg/dL (>13.9 mmol/L). The observation was terminated when the mice were 30 weeks old. Statistical analysis was performed by Log-rank test.

Fig. 2 - The composition of gut microbiota in *Nod2*$^{-/-}$NOD mice is dependent on housing status

Bacterial DNA was extracted from fecal pellets from non-cohoused and cohoused 12-week old *Nod2*$^{-/-}$NOD and *Nod2*$^{+/+}$NOD female mice (n=5-6/group, randomly selected from the mice in Fig. 1C) and used for pyrosequencing. Principal component analysis (unweighted) of beta diversity of the gut microbiota in *Nod2*$^{+/+}$NOD and *Nod2*$^{-/-}$NOD female mice is shown for non-cohoused (Fig. 2A) and cohoused (Fig. 2B) mice. The composition of gut microbiota was compared at genus level between *Nod2*$^{-/-}$NOD and *Nod2*$^{+/+}$NOD mice (n=6 each) which were cohoused (CH) or non-cohoused (NCH) (Fig. 2C-G). The abundance of SFB in the gut microbiota was assessed by qPCR with SFB specific primers (Fig. 2H).

The level of SFB expression was calculated by the delta-delta threshold cycle method after normalization with bacterial 16S rRNA. Each sample was plated in triplicate and the experiments were repeated twice. Student's t test was used for statistical analysis (*P<0.05; **P<0.001). Error bars represent SEM.

Fig. 3 - Cohousing affects IgA, IgG2b and IgG1 secreting B-cells in the PP and gut lumen

(A), IgA secreting B-cells ($CD19^+IgA^+$ B-cells) in the Peyer's patches were investigated in 12-week old female *Nod2*$^{-/-}$NOD and *Nod2*$^{+/+}$NOD mice using flow cytometry. Left: A set of representative FACS plots. Right: The graphical summary of the IgA-secreting B-cells in the 4 groups (n=8, pooled from two independent experiments). (B), IgA concentration in the small intestine of *Nod2*$^{-/-}$NOD and *Nod2*$^{+/+}$NOD mice cohoused (CH) or non-cohoused (NCH) was measured by ELISA. Data for (B) are from 3 individual experiments (n=7-8). (C) and (D) IgG2b-secreting B-cells and IgG1-secreting B-cells in the Peyer's patches were investigated in 12-week old female *Nod2*$^{-/-}$NOD and *Nod2*$^{+/+}$NOD mice using flow cytometry (n=4). Student's t test was used for statistical analysis. *P<0.05, **P<0.01. Error bars represent SEM.

Fig. 4 - Cytokine-producing $CD4^+$ and $CD8^+$ T-cells are altered by the absence of Nod2 and the cohousing conditions

Intracellular staining was conducted on T cells from the spleen, pancreatic lymph nodes (PLN) and Peyer's patches (PP) from 12-week old female *Nod2*$^{-/-}$NOD (KO) and

Nod2$^{+/+}$NOD mice in both cohoused (CH) and non-cohoused (NCH) conditions. (A), The percentages of IFNγ-producing CD8^{+} T-cells and (B), IL-17a-producing CD4^{+} T-cells. The data represent at least 3 independent experiments (n=3-4/group/experiment). Student's t test was used for statistical analysis. *P<0.05; **P<0.001; *** P<0.0001. Error bars represent SEM.

Fig. 5 –Treg proportion and function is affected by cohousing

Intracellular staining was conducted on T-cells from the spleen, pancreatic lymph nodes (PLN), mesenteric lymph nodes (MLN) and Peyer's patches (PP) from 12-week old female *Nod2*$^{-/-}$ NOD (KO) and *Nod2*$^{+/+}$NOD mice in both cohoused (CH) and non-cohoused (NCH) conditions. (A), Representative Treg FACS plots shown for each group (gated on Live single B220-TCRbeta+CD8a-CD4+CD25+FoxP3+ cells). (B), Compiled data from A, (n=6-8). Pancreatic lymph node CD4+CD25+ Tregs were isolated using magnetic beads from 12-week old *Nod2*$^{+/+}$NOD and *Nod2*$^{-/-}$NOD KO mice in both cohoused and non-cohoused conditions and mitomycin-c-treated (20mins, 37°C). NOD Splenic T cells were depleted using complement to enrich APCs, which were then mitomycin-c treated (100,000/well). Isolated splenic T-cells from 12 week-old C57BL/6 mice were isolated and co-cultured with Tregs at a ratio of 1:3 (Treg:Tresponder) for 5 days, prior to supernatant collection and thymidine addition for the last 18 hours. (C), Proliferation suppression was calculated by (100-proliferation)/control x 100. Control was defined as the proliferation when no Tregs were added. (D), Supernatants were tested for the

concentration of IL-10 by ELISA. Data shown are pooled from two independent experiments. Statistical analysis was performed using Student t test, *P<0.05; **P<0.0001.

Fig. 6 - The direct effect of gut microbiota on immune cells

Gut bacteria from the large intestine of *Nod2*$^{-/-}$NOD or *Nod2*$^{+/+}$NOD mice were harvested and used to stimulate splenocytes (5×10^6/ml) from *Nod2*$^{-/-}$NOD or *Nod2*$^{+/+}$NOD mice with or without heat-inactivated gut bacteria (10^8 cfu) for 14 hours. The expression of IFN-γ in CD8$^+$ T-cells (A) and IL-17A (B) in CD4$^+$ T-cells was assessed by intracellular cytokine staining. Representative FACS plots are shown on the top. The results are pooled from three independent experiments. Student's t test was used for statistical analysis. * P<0.05; **, P<0.001; ***, P<0.0001. * Data comparison was between cells incubated with no bacteria (control) and either *Nod2*$^{-/-}$NOD or *Nod2*$^{+/+}$NOD derived bacteria (A and B) or between *Nod2*$^{-/-}$NOD or *Nod2*$^{+/+}$NOD derived bacteria stimulation (A).

Fig. 7 – Colonization of GF NOD with bacteria alters immune cell cytokine secretion and function

GF NOD mice were gavaged once with $2x10^8$ CFU fecal bacteria from 4-5 week old KO *Nod2*$^{-/-}$NOD or *Nod2*$^{+/+}$NOD mice. Bacterial DNA was extracted from fecal pellets from WT or KO gavaged ex-GF NOD mice (n=7/group) and the original bacteria donors. Pyrosequencing was conducted using the Ion Torrent PGM sequencing system. The

sequencing data were analyzed with QIIME software package and UPARSE pipeline to pick operational taxonomic units (OTUs). Taxonomy assignment was performed at phylum level using representative sequences of each OTU. Principal component analysis (unweighted) of beta diversity of the gut microbiota from WT gavaged and KO gavaged mice is shown (A). 2-3 weeks later mice were sacrificed for immunophenotyping. Intracellular staining was conducted on B-cells (gated on live single TCRbeta-$CD11b^{-}CD11c^{-}B220^{+}$) and T-cells (gated on live single $TCRbeta^{+}B220^{-}$ cells then CD4 or CD8) from the pancreatic lymph nodes (B). FoxP3 staining was conducted following the instructions from the eBioscience staining kit for cells from spleen, pancreatic lymph nodes (PLN), mesenteric lymph nodes (MLN) and Peyer's patches (PP). Cells were gated on live single $B220^{-}TCRbeta^{+}CD8a^{-}CD4^{+}CD25^{+}FoxP3^{+}$ cells (C). Absolute numbers were calculated for MLN (D) and PP (E) Treg cells. All data shown are pooled from two independent experiments (n=3-4/experiment). Statistical analysis was performed using Student's t test, *$P<0.05$ or **$P<0.0001$. Lines represent the mean and the standard deviation.

Fig. 1

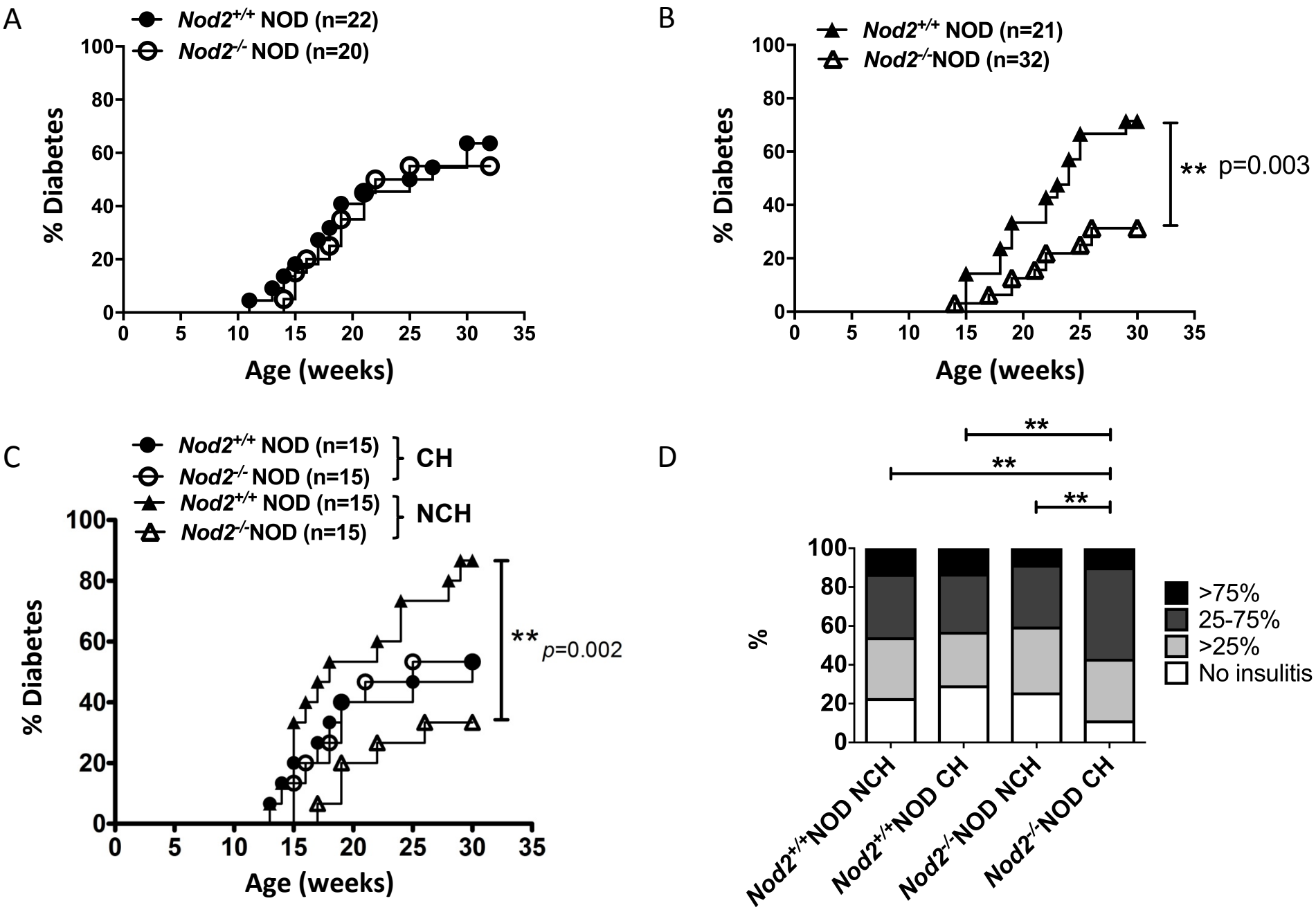
A
Nod2+/+ NOD (n=22)
Nod2-/- NOD (n=20)
% Diabetes
Age (weeks)
B
Nod2+/+ NOD (n=21)
Nod2-/-NOD (n=32)
% Diabetes
** p=0.003
Age (weeks)
C
Nod2+/+ NOD (n=15)
Nod2-/- NOD (n=15)
CH
Nod2+/+ NOD (n=15)
Nod2-/-NOD (n=15)
NCH
% Diabetes
** p=0.002
Age (weeks)
D
**
**
**
%
>75%
25-75%
>25%
No insulitis
Nod2+/+NOD NCH
Nod2+/+NOD CH
Nod2-/-NOD NCH
Nod2-/-NOD CH

Fig. 2

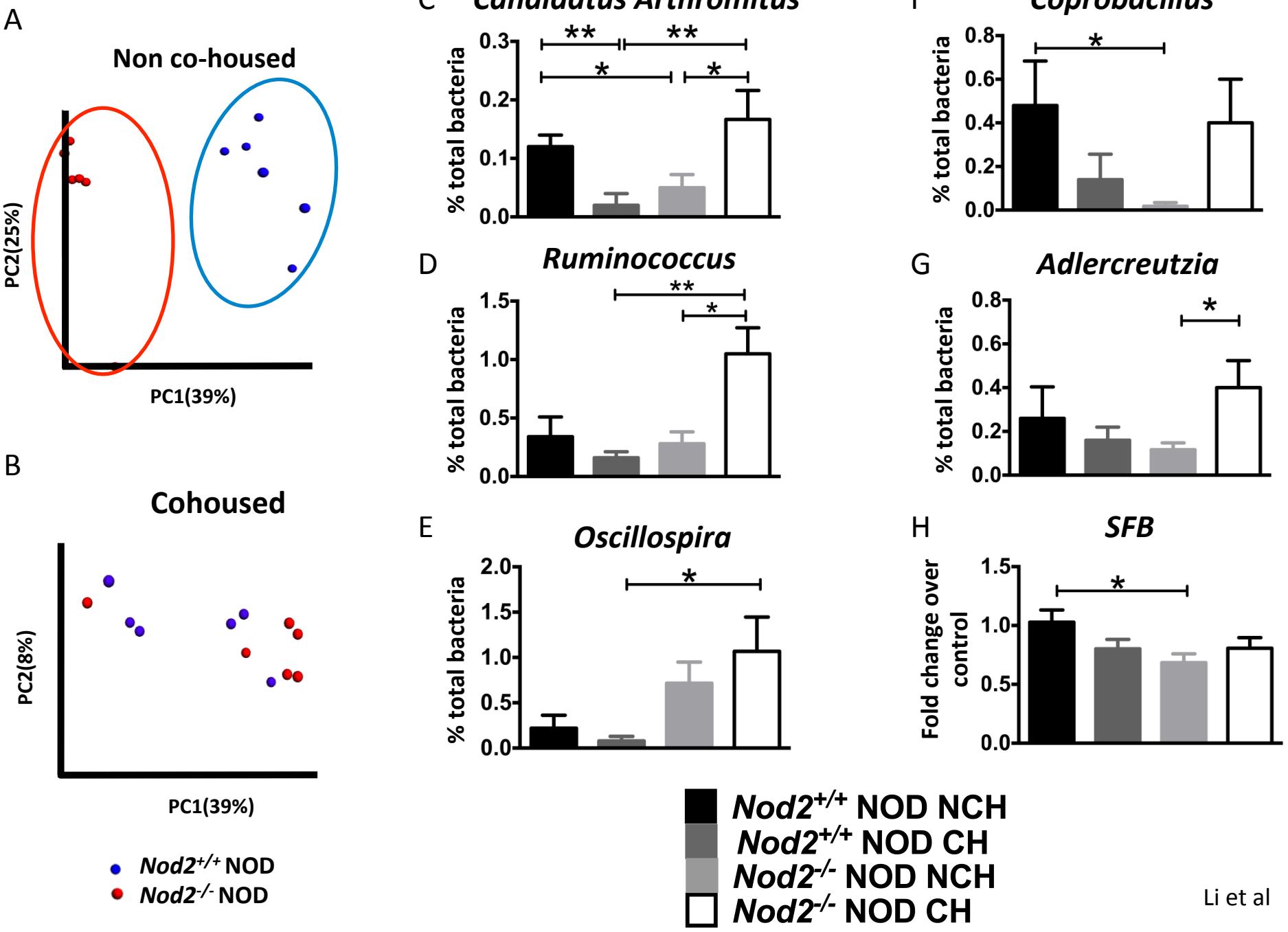
A
Non co-housed
PC2(25%)
PC1(39%)
B
Cohoused
PC2(8%)
PC1(39%)
Nod2+/+ NOD
Nod2-/- NOD
C
Candidatus Arthromitus
% total bacteria
D
Ruminococcus
% total bacteria
E
Oscillospira
% total bacteria
F
Coprobacillus
% total bacteria
G
Adlercreutzia
% total bacteria
H
SFB
Fold change over control
Nod2+/+ NOD NCH
Nod2+/+ NOD CH
Nod2-/- NOD NCH
Nod2-/- NOD CH

Li et al

Fig. 3

Li et al

A

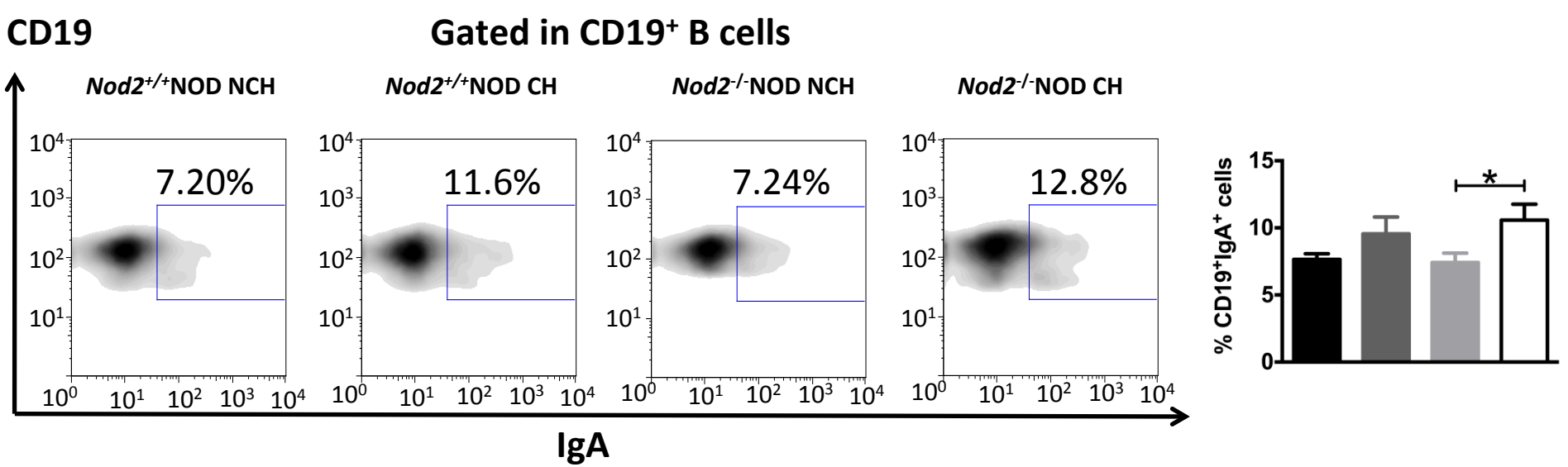

B

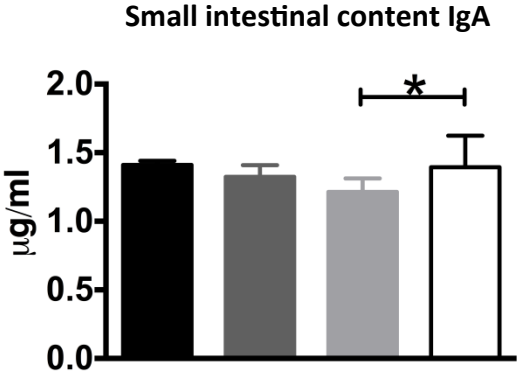

C

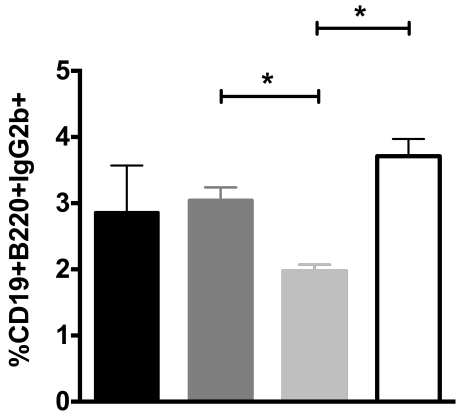

D

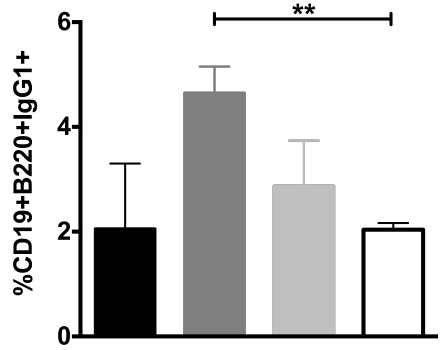

Nod2+/+ NOD NCH
Nod2+/+ NOD CH
Nod2-/- NOD NCH
Nod2-/- NOD CH

Fig. 4

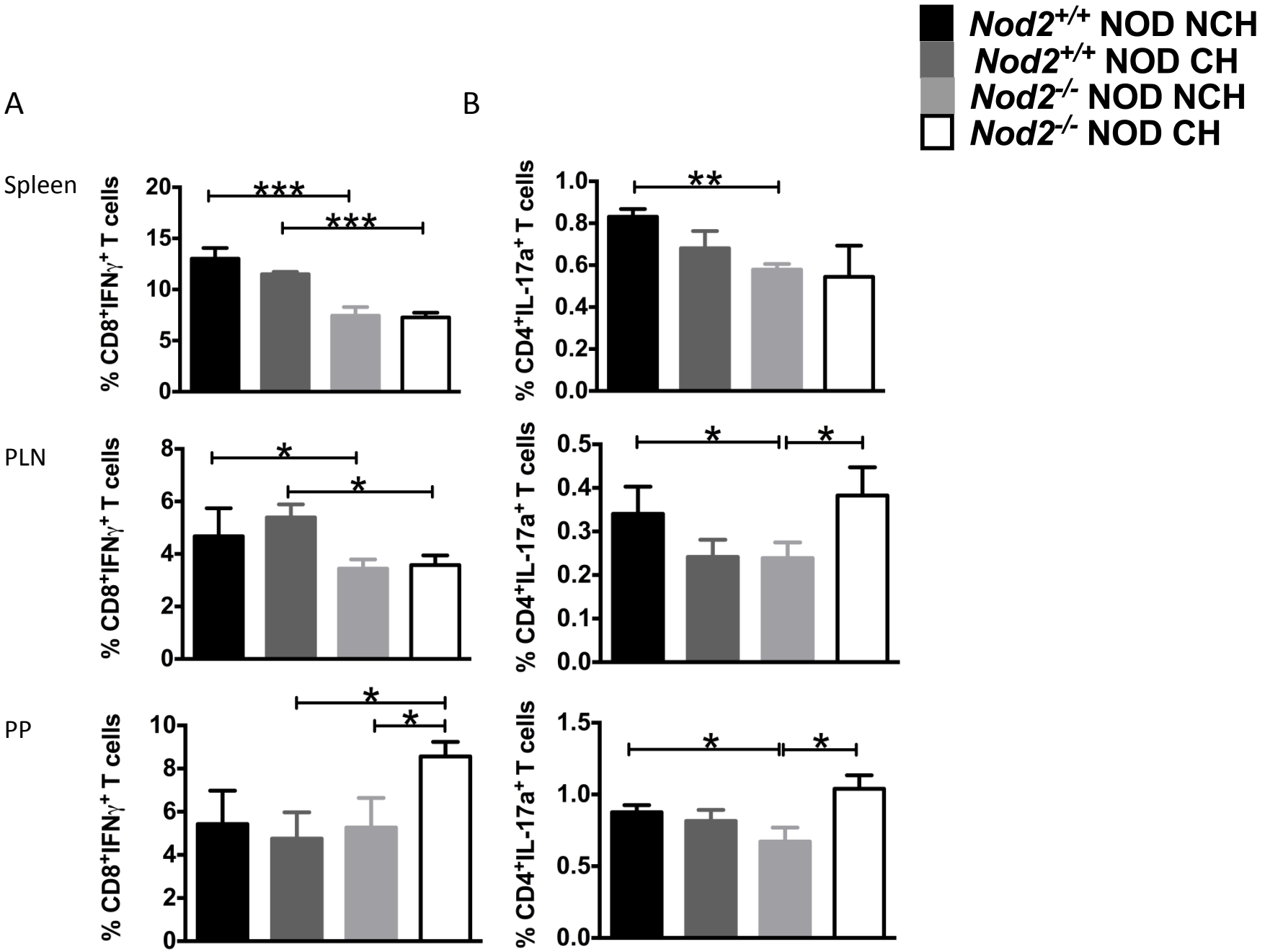
Nod2+/+ NOD NCH
Nod2+/+ NOD CH
Nod2-/- NOD NCH
Nod2-/- NOD CH
A
B
Spleen
PLN
PP
% CD8+IFNγ+ T cells
% CD4+IL-17a+ T cells
***
**
*

Li et al

Fig. 5

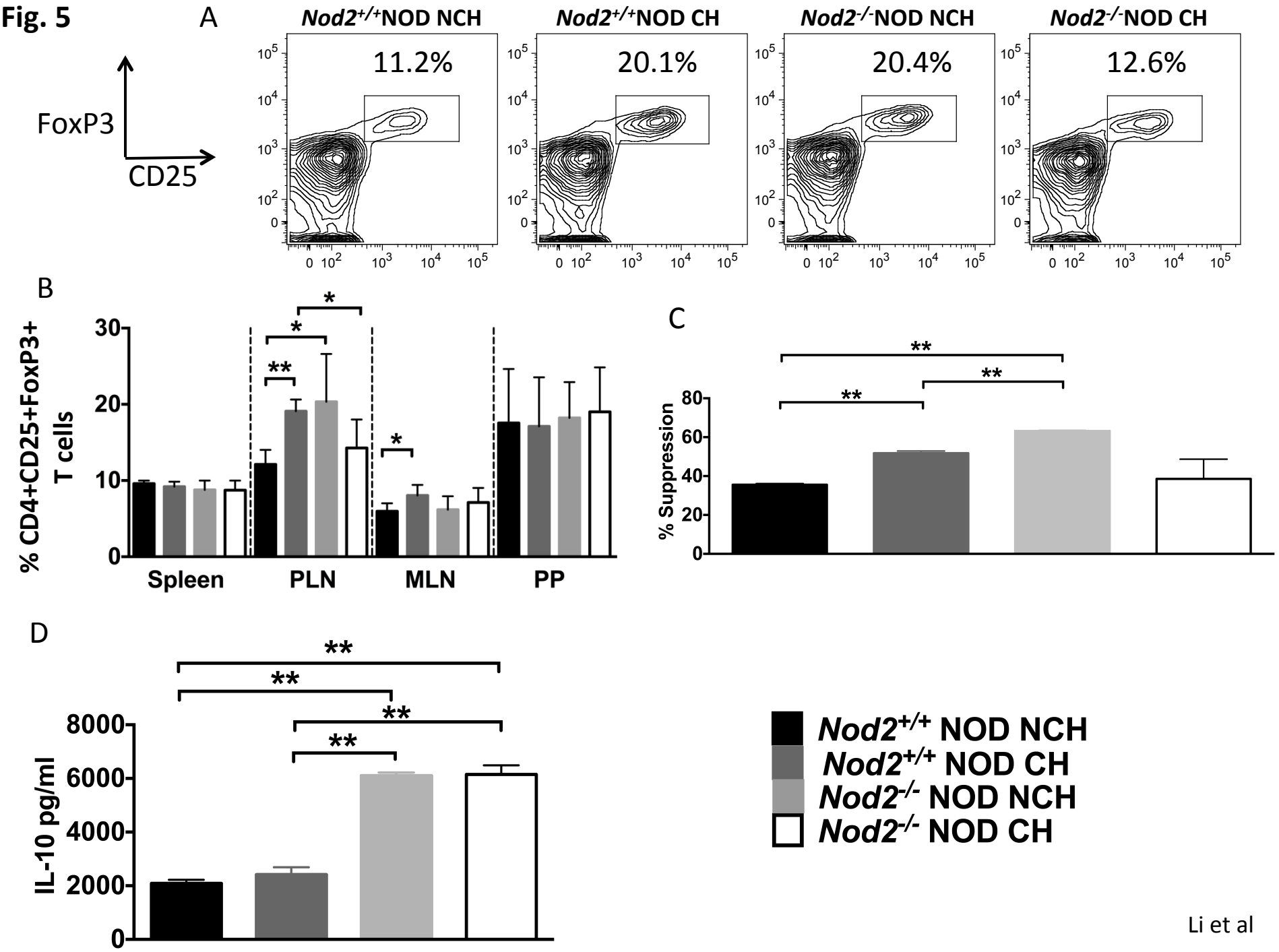
A
Nod2+/+NOD NCH
Nod2+/+NOD CH
Nod2-/-NOD NCH
Nod2-/-NOD CH
FoxP3
CD25
11.2%
20.1%
20.4%
12.6%
B
% CD4+CD25+FoxP3+ T cells
Spleen
PLN
MLN
PP
C
% Suppression
D
IL-10 pg/ml
Nod2+/+ NOD NCH
Nod2+/+ NOD CH
Nod2-/- NOD NCH
Nod2-/- NOD CH

Li et al

Fig. 6

Li et al

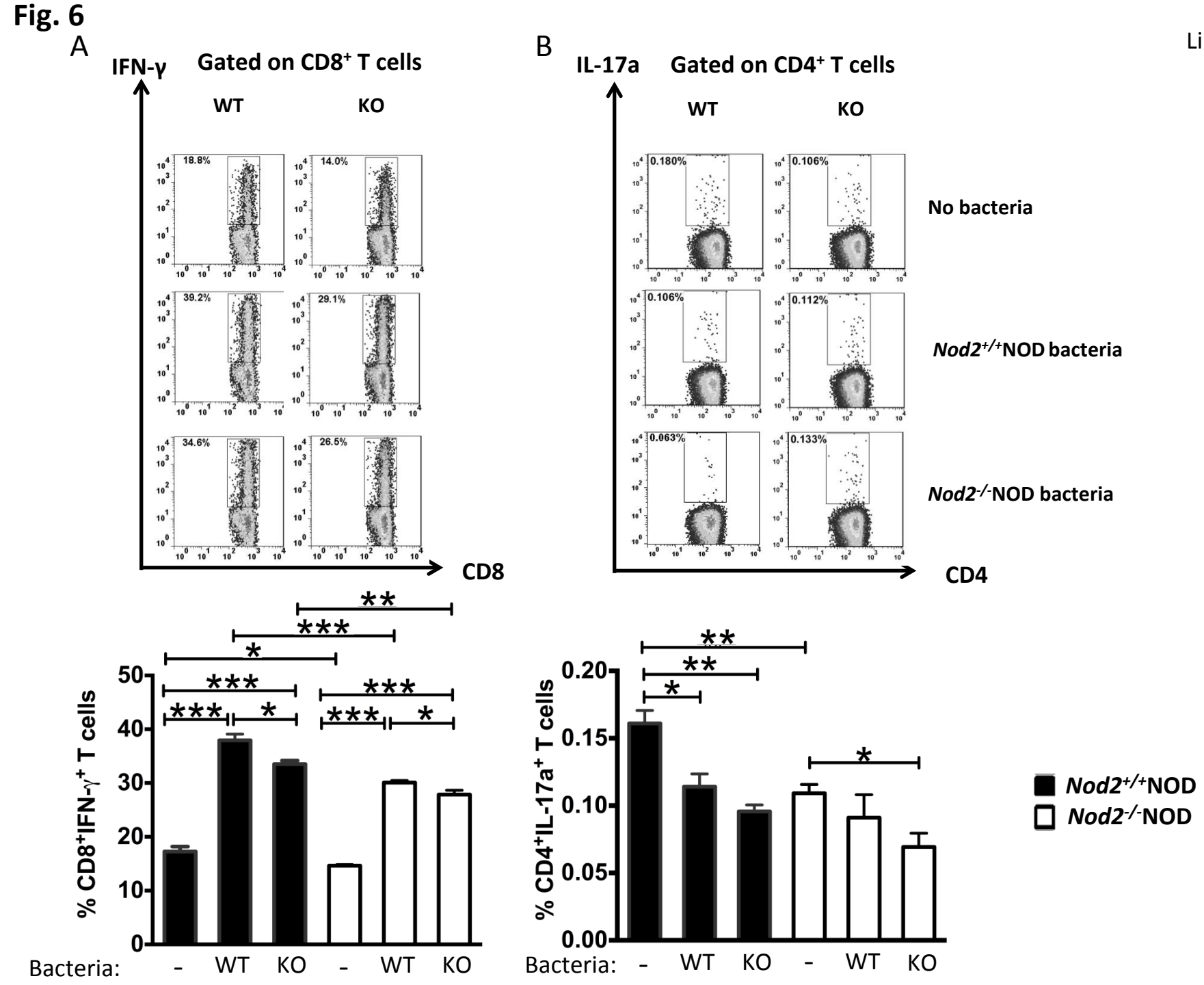
A
IFN-γ
Gated on CD8+ T cells
WT
KO
18.8%
14.0%
39.2%
29.1%
34.6%
26.5%
CD8
B
IL-17a
Gated on CD4+ T cells
WT
KO
0.180%
0.106%
0.106%
0.112%
0.063%
0.133%
No bacteria
Nod2+/+NOD bacteria
Nod2-/-NOD bacteria
CD4
% CD8+IFN-γ+ T cells
Bacteria: - WT KO - WT KO
% CD4+IL-17a+ T cells
Bacteria: - WT KO - WT KO
Nod2+/+NOD
Nod2-/-NOD

Fig. 7

Li et al

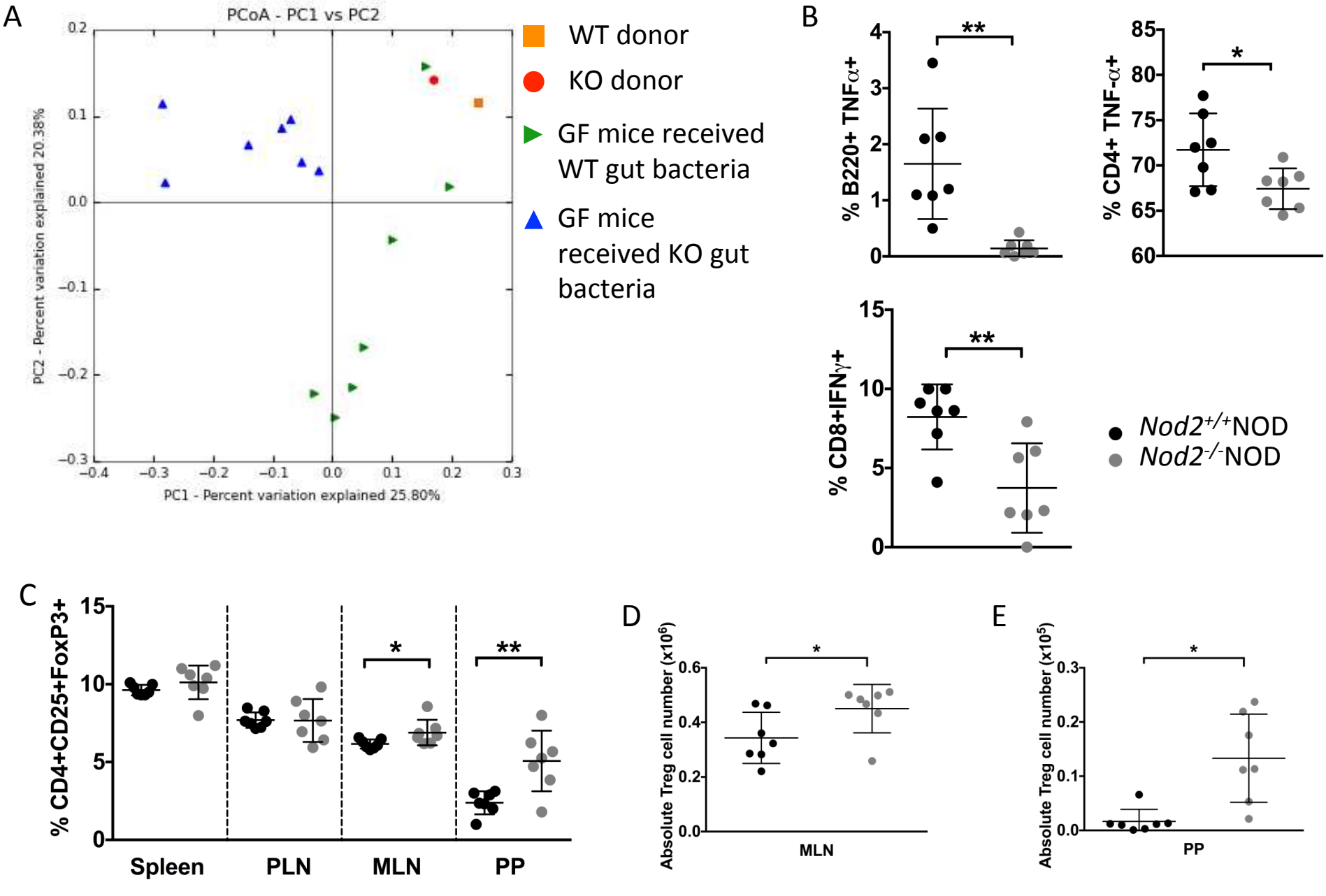
A
PCoA - PC1 vs PC2
PC2 - Percent variation explained 20.38%
PC1 - Percent variation explained 25.80%
WT donor
KO donor
GF mice received WT gut bacteria
GF mice received KO gut bacteria
B
% B220+ TNFα+
% CD4+ TNF-α+
% CD8+IFNγ+
Nod2+/+NOD
Nod2-/-NOD
C
% CD4+CD25+FoxP3+
Spleen
PLN
MLN
PP
D
Absolute Treg cell number (x10^6)
MLN
E
Absolute Treg cell number (x10^5)
PP

Supplemental Figure Legends

Supplemental Fig. 1 – Nod2 and cohousing alter the gut microbiota and antimicrobial peptide expression

(A) Bacterial DNA was extracted from fecal pellets from *Nod2*$^{+/+}$NOD homozygous and *Nod2*$^{-/-}$NOD homozygous breeder litters at 3 weeks of age (prior to changes in housing) and 8-9-weeks of age from cohoused (CH) and non-cohoused (NCH) *Nod2*$^{-/-}$NOD and *Nod2*$^{+/+}$NOD female mice (n=4-8/group, selected from the mice in Fig. 1C) and used for pyrosequencing. Principal component analysis (unweighted) of beta diversity of the gut microbiota in cohoused and non-cohoused *Nod2*$^{+/+}$NOD and *Nod2*$^{-/-}$NOD female mice is shown (A). (B-D) Distal small intestinal RNA from 13-14-week old *Nod2*$^{-/-}$NOD and *Nod2*$^{+/+}$NOD female mice (cohoused and non-cohoused) was used to generate cDNA. QPCR was then conducted for the antimicrobial peptides (Reg3γ, Reg3β and RelmB). Samples were compared to GAPDH and fold change was generated from ΔΔCT values. Statistical analysis was performed using Student t test; *P<0.05 or **P<0.01.

Supplemental Fig. 2 - Nod2 deficiency does not alter the function of DC or macrophages

Antigen presenting function of *Nod2*$^{-/-}$NOD mice was tested *in vitro* (A, B) and *in vivo* (C). Splenic macrophages (Mϕ) (CD11b^{+}) and DC (CD11c^{+}) cells, from *Nod2*$^{-/-}$NOD and *Nod2*$^{+/+}$NOD mice, were purified with purification kits (Stem Cell Technology) and co-cultured (10^4) with purified CD4^{+} T-cells (10^5) from BDC2.5 TCR transgenic NOD mice (A) or CD8^{+} T-cells (10^5) from NY8.3 TCR transgenic NOD mice (B) in the presence or

absence of BDC2.5 mimotope peptide or $IGRP_{206-214}$ peptide at various concentrations for 72 hours before adding thymidine (^3H). The cells were harvested 18 hours later; thymidine incorporation was measured by beta-counter. Data are shown as counts per minute (cpm) after subtraction of the background (~200 – 1,000 cpm).

To test the antigen presenting function, *in vivo*, splenic T-cells from *Nod2*$^{-/-}$NOD mice and *Nod2*$^{+/+}$NOD mice were transferred (10^7/mouse) into immunodeficient NOD.scid (*Nod2*$^{+/+}$NOD.scid) or *Nod2*$^{-/-}$NOD.scid recipients. Mice were screened daily post-transfer for glycosuria and diabetes development confirmed with a blood glucose level $\geq$250mg/dl (C).

Supplemental Fig. 3 – Reconventionalized GF NOD mice exhibit increased cecal weight and B cells with reduced antigen presenting capabilities

GF NOD mice were gavaged once with $2x10^8$ CFU fecal bacteria from 4-5 week old *Nod2*$^{+/+}$NOD or *Nod2*$^{-/-}$NOD mice. 2-3 weeks post gavage, mice were sacrificed and cecal weights (A) were measured. Splenic B-cells were isolated from the mice using magnetic beads and subsequently mitomycin-c treated. BDC2.5 $CD4^+$ (B) and NY8.3 $CD8^+$ (C) T-cells were isolated from BDC2.5 and NY8.3 transgenic mice, respectively, and co-cultured at a 1:1 ratio with B-cells and mimotope/peptide. Cells were cultured for 48 hours and thymidine was added to assess cell proliferation for the last 18 hours. Data are shown after subtraction of background (cpm ~350-800) and are pooled from two independent

experiments (n=3-4/experiment). Statistical analysis was performed using Student t test; **P<0.0001 (B) or two way ANOVA; **P<0.0001 (C and D).

Supplemental Fig. 1

Li et al

A

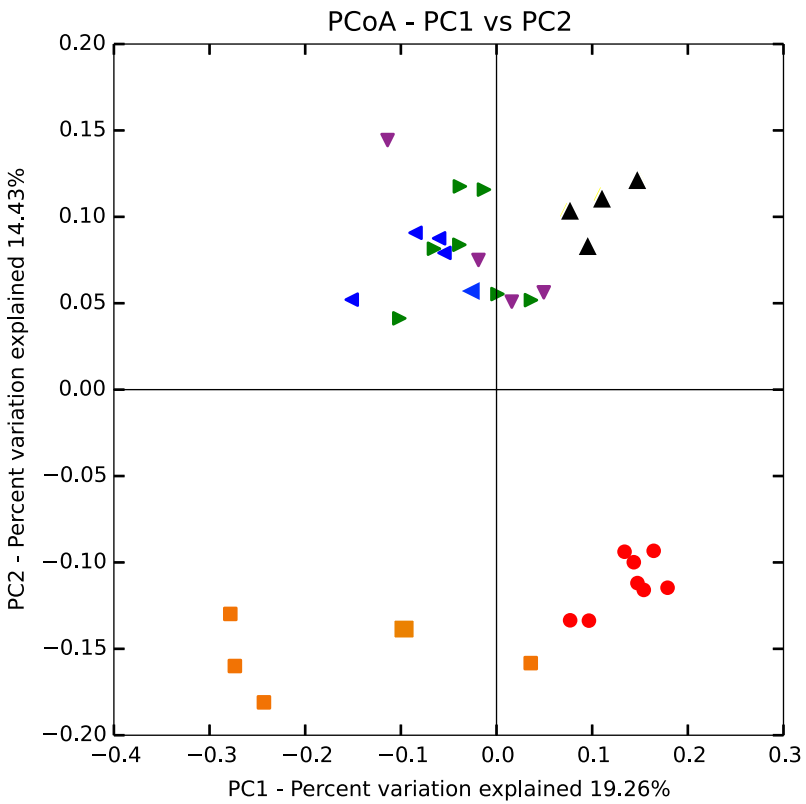

- *Nod2*$^{+/+}$NOD – 3 weeks of age
- *Nod2*$^{+/+}$NOD NCH – 8-9 weeks of age
- *Nod2*$^{+/+}$NOD CH – 8-9 weeks of age
- *Nod2*$^{-/-}$NOD – 3 weeks of age
- *Nod2*$^{-/-}$NOD NCH – 8-9 weeks of age
- *Nod2*$^{-/-}$NOD CH – 8-9 weeks of age

B

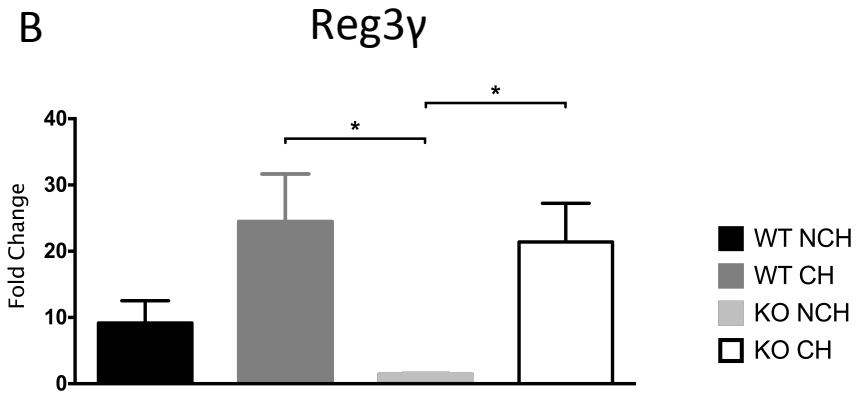

C

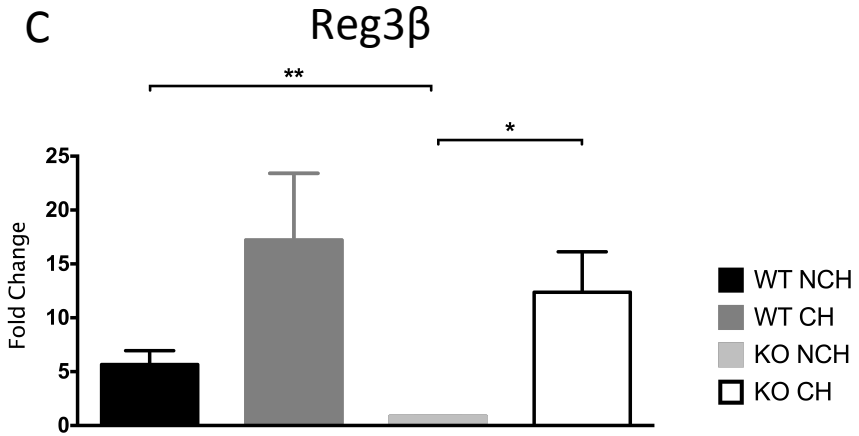

D

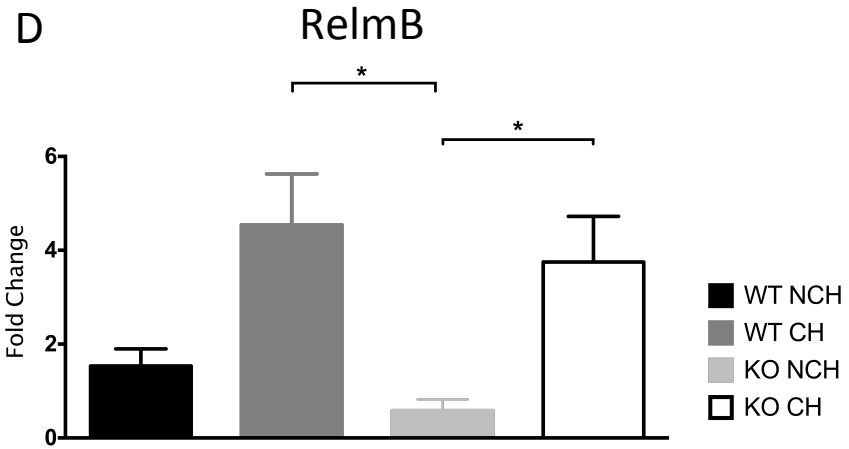

Supplemental Fig. 2

Li et al

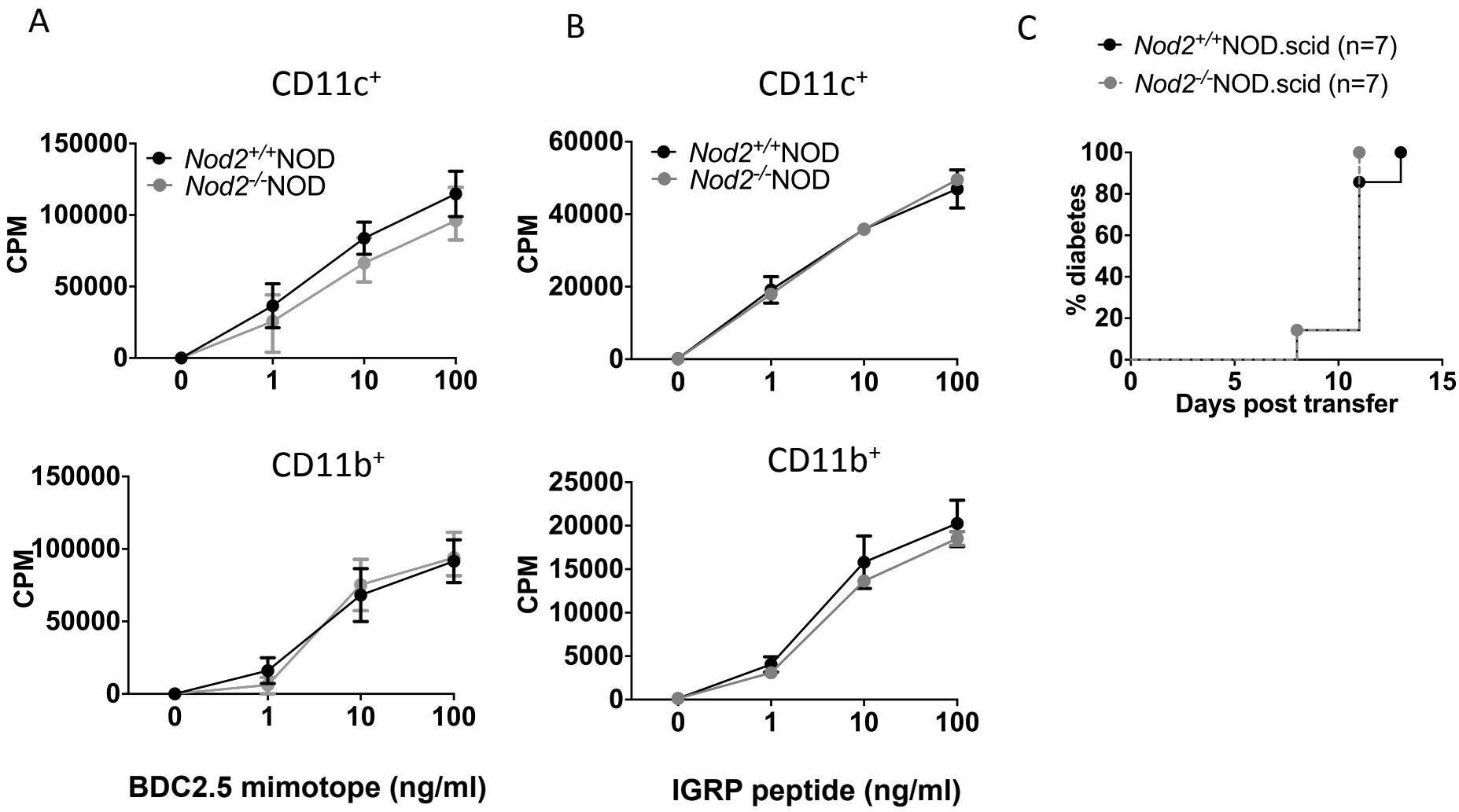

Supplemental Fig. 3

Li et al

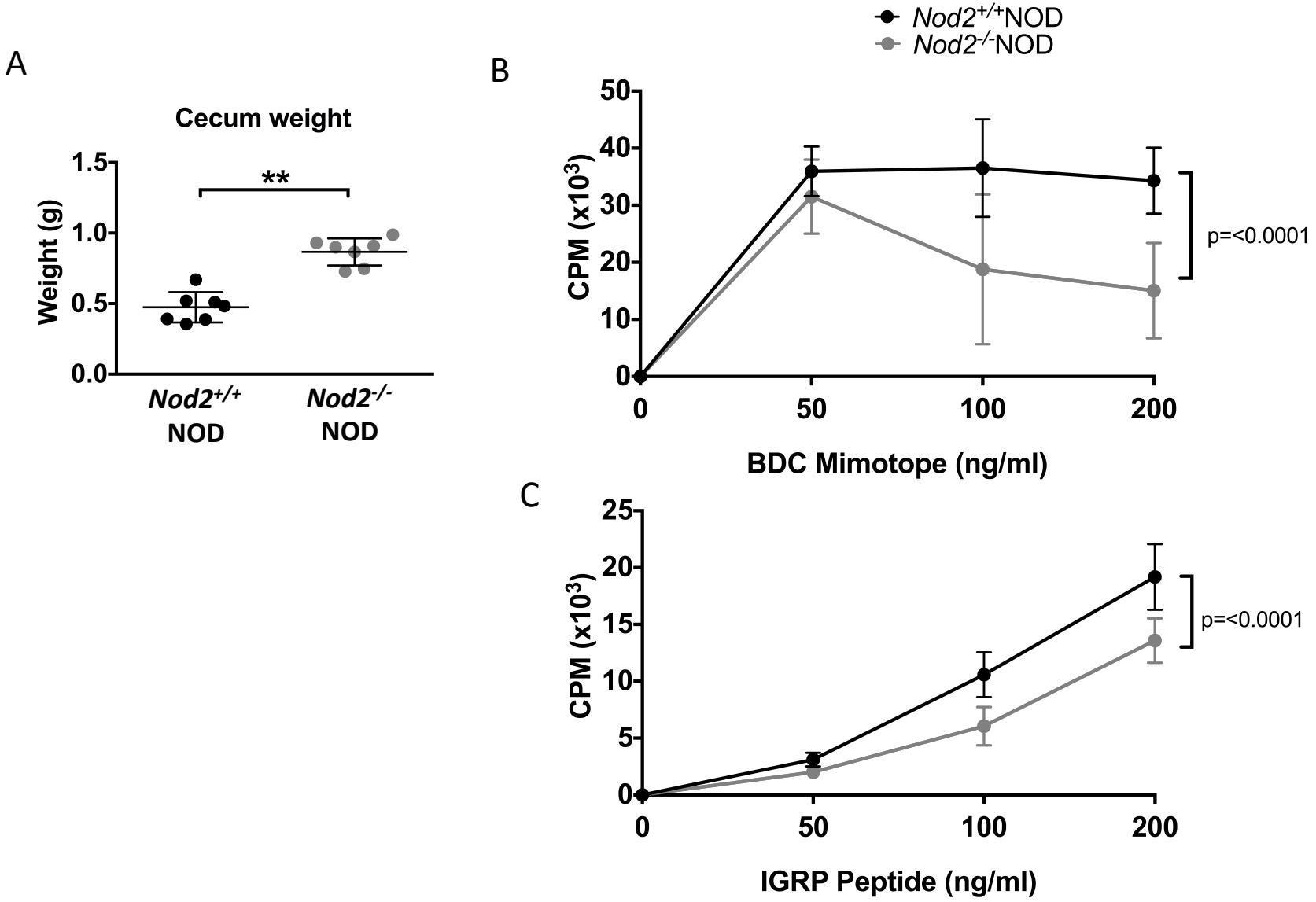

Supplemental Information

Supplementary Table 1 – Summary of Mouse Breeding and observation cohorts

Group	Breeding	Housing Partners (from birth)	Housing Partners (post-weaning)	Gut Microbiota	Incidence of Diabetes	Related Figures
1	*Nod2*$^{+/-}$ x *Nod2*$^{+/-}$	*Nod2*$^{-/-}$ and *Nod2*$^{+/+}$	*Nod2*$^{-/-}$ and *Nod2*$^{+/+}$	Shared	Similar	Figure 1A (CH)
2	*Nod2*$^{+/-}$ x *Nod2*$^{+/-}$	*Nod2*$^{-/-}$ and *Nod2*$^{+/+}$	Housed by genotype	Different	*Nod2*$^{-/-}$ have reduced diabetes vs *Nod2*$^{+/+}$	Figure 1B (NCH)
3	*Nod2*$^{-/-}$ x *Nod2*$^{-/-}$	*Nod2*$^{-/-}$	*Nod2*$^{-/-}$	Different	NCH *Nod2*$^{-/-}$ have reduced diabetes vs NCH *Nod2*$^{+/+}$	Figure 1C (CH and NCH)
4	*Nod2*$^{+/+}$ x *Nod2*$^{+/+}$	*Nod2*$^{+/+}$	*Nod2*$^{+/+}$	Different	NCH *Nod2*$^{-/-}$ have reduced diabetes vs NCH *Nod2*$^{+/+}$	Figure 1C (CH and NCH)

CH = Cohoused - both genotypes in each cage (*Nod2*$^{+/+}$ and *Nod2*$^{-/-}$)

NCH = Non-cohoused - One genotype in each cage (*Nod2*$^{+/+}$ or *Nod2*$^{-/-}$)